Electronic Supplementary Information

Cholesterol oxidase-immobilized MXene/sodium alginate/silica@*n*-docosane hierarchical microcapsules for ultrasensitive electrochemical biosensing detection of cholesterol†

Meng Zhang, Huan Liu,* Xiaodong Wang*

State Key Laboratory of Organic–Inorganic Composites, Beijing University of Chemical Technology, Beijing 100029, China

* Corresponding authors.

E-mail: bucthuan@163.com (H. Liu); wangxdfox@aliyun.com (X. Wang).

Summary of Content

Section S1. Synthesis of $Ti_3C_2T_x$ MXene nanosheets.

$Ti_3C_2T_x$ MXene nanosheets (T_x represents −F or −OH) were synthesized through selective etching of Al layers from the Ti_3AlC_2 powders using an *in-situ* HF-etching method, followed by ultrasonic exfoliation according to the method depicted in **Scheme S1**. In a typical procedure, LiF (1.0 g) was dissolved in HCl solution (20 mL, 37 wt %) to form an etching solution in a plastic beaker. Then, Ti_3AlC_2 (1.0g) was slowly immersed in the HF etching solution under continuous agitation at room temperature for 48 h. After that, the resultant mixed solution was washed with deionized water several times *via* centrifugation until a neutral pH level was obtained. Finally, a suspension containing $Ti_3C_2T_x$ MXene nanosheets was obtained through ultrasonic exfoliation under an argon flow of 20 mL·min^{-1}, followed by centrifugation at 3500 rpm for 1 h.

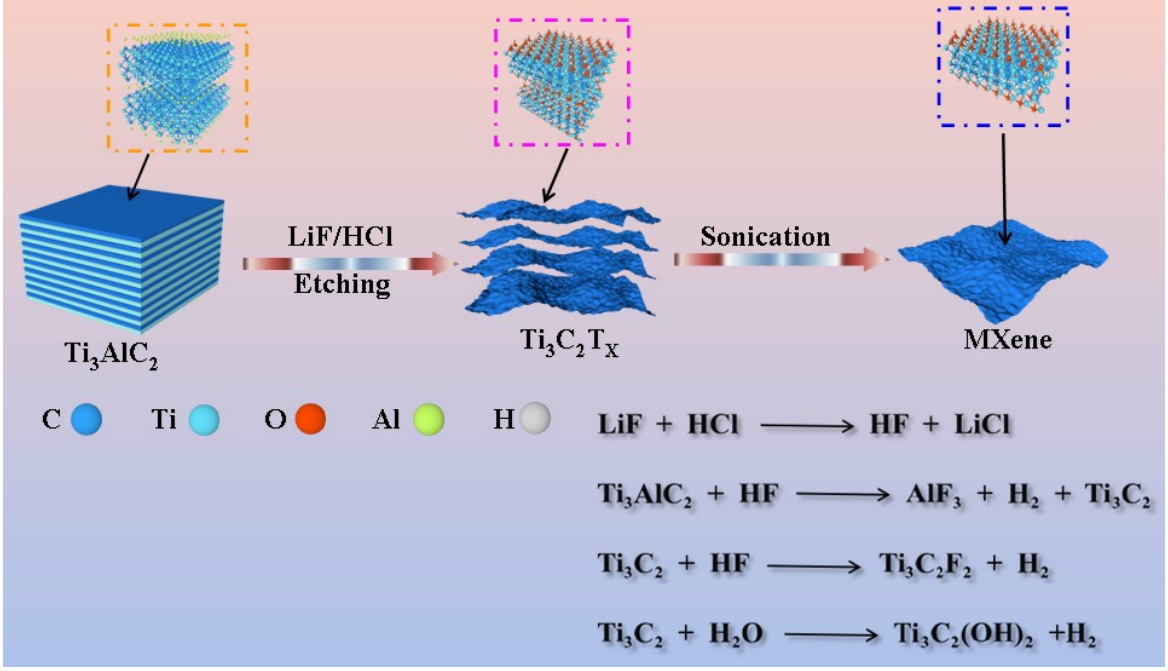

Scheme S1 Schematic synthetic route for $Ti_3C_2T_x$ MXene nanosheets.

Section S2. Characterizations and measurements

The morphologies of microcapsule samples were characterized using a Zeiss SUPRA™ 55 scanning electron microscope (SEM) at an acceleration voltage of 20 kV. The resultant SEM micrographs were analyzed with the Nano Measure™ software to determine the size distributions and average diameters of microcapsule samples. The microstructure of microcapsule samples was characterized using a JEOL JEM 2100 transmission electron microscope (TEM) at an acceleration voltage of 100 kV. *X*–ray powder diffraction (XRD) patterns were recorded on a Japan Rigaku D/max 2500VB2+/PC *X*–ray diffractometer using a Cu–Kα radiation source. Surface elemental distribution and the corresponding mapping images were obtained with an Oxford INCAX-Act energy-dispersive *X*–ray (EDX) spectrometer equipped on the SEM instrument. X–ray photoelectron (XPS) spectroscopy was conducted using a Thermo Fisher ESCALAB–250 XPS spectrometer equipped with a focused monochromatized Al–Kα radiation source (1486.6 eV) to confirm the atomic states of the shell materials of the microcapsules. The survey spectrum of powder specimen was acquired at 200 eV pass energy, while the core level spectra were performed setting the pass energy at 30 eV and a step size of 0.05 eV. The detection spot size was determined as 500 μm. The C 1s with the main peak at 284.8 eV corresponding to *n*-docosane was used as the internal reference to calibrate the survey spectrum. The core level XPS spectra were fitted through the XPSPEAK41 software, in which a Shirley background was assumed. The Lorentzian-Gaussian peak shape was used to optimize the core level XPS spectra deconvolution. *Fourier*-transform infrared (FTIR) spectra were recorded on a Thermo Scientific Nicolet iS5 infrared spectrometer in the wavelength range of 400–4000 cm^{-1} at a resolution of 2 cm^{-1}. Ultraviolet–visible (UV–Vis) spectra were collected using a Lambda 35 UV spectrophotometer (Perkin Elmer Corp., USA). A microcapsule sample (around 20 mg) was dispersed in deionized water (10 mL) by sonification, and the resulting suspension (about 3.5 mL) was taken for the test.

Phase-change behaviors and thermal parameters were determined by differential scanning calorimetry (DSC) using a TA Instruments Q20 differential scanning calorimeter. A ramp rate of 10 ºC/min under a nitrogen flux was employed, and indium was used as a standard to calibrate the changes of phase-change temperature and enthalpy. Melting peak temperature (T_m) and crystallization peak temperature (T_c) were

directly read from the DSC thermogram, while melting enthalpy (ΔH_m), and crystallization enthalpy (ΔH_c) were determined from the definite integral of endothermic and exothermic peaks in the DSC thermogram, respectively. DSC measurement was performed five times for each sample, and the reported data represented an average value from five tests. Moreover, encapsulation ratio (E_{en}), energy-storage efficiency (E_{es}), and energy-storage capability (C_{es}) as three important encapsulation parameters for microcapsule samples were determined from the DSC analysis data using the following equations.

$$E_{en}(\%) = \frac{\Delta H_{m,\,MEPCM}}{\Delta H_{m,\,PCM}} \times 100\% \tag{1}$$

$$E_{es}(\%) = \frac{\Delta H_{m,\,MEPCM} + \Delta H_{c,\,MEPCM}}{\Delta H_{m,\,PCM} + \Delta H_{c,\,PCM}} \times 100\% \tag{2}$$

$$C_{es}(\%) = \frac{(\Delta H_{m,\,MEPCM} + \Delta H_{c,\,MEPCM}) \cdot \Delta H_{m,\,PCM}}{(\Delta H_{m,\,PCM} + \Delta H_{c,\,PCM}) \cdot \Delta H_{m,\,MEPCM}} \times 100\% \tag{3}$$

where $\Delta H_{c,\,PCM}$ and $\Delta H_{m,\,PCM}$ are the crystallization and melting enthalpies of pure *n*-docosane, respectively, and $\Delta H_{c,\,MEPCM}$ and $\Delta H_{m,\,MEPCM}$ represent the crystallization and melting enthalpies of microcapsule samples, respectively. Thermogravimetric analysis (TGA) was performed using a TA Instruments Q50 thermogravimetric analyzer under a nitrogen flux. A heating rate of 10 ºC/min was used, and sample weights were between 3.0 and 5.0 mg.

The immobilization amount of cholesterol oxidase (Chox) on the microcapsules was determined using a UV spectrometric method. In a typical procedure, 1.0 mg of Chox-immobilized microcapsules and 5 mL of cholesterol solution (1 mM) were mixed in 10 mL of PBS (pH = 7.0) under agitation for 5 min at room temperature. This allows cholesterol to undertake an enzyme-catalytic redox reaction to produce cholestenone. The obtained reactant solution was transferred to a sample cell immediately, and its UV absorbance spectrum was recorded using the Lambda 35 UV spectrophotometer. In the recorded UV-Vis spectrum, the absorbance band at a wavelength of around 240 nm is associated with the produced cholestenone. Meanwhile, the UV-Vis spectrum of the cholesterol solution without the Chox-immobilized microcapsules was recorded on the same spectrophotometer. The enzyme activity (*E.A.*) of the immobilized Chox could be determined using the

following equation:

$$E.A.\ (\mathrm{U/g}) = \frac{(A_t - A_0) \times 10^6 \times V_t}{\varepsilon \times t \times m} \tag{4}$$

where A_0 and A_t are the absorbance intensities of cholestenone at 240 nm before and after the enzyme-catalytic redox reaction, respectively, V_t the volume of reaction system, ε the molar extinction coefficient of cholestenone (12200 $M^{-1} \cdot cm^{-1}$), t the reaction time, and m is the mass of the Chox-immobilized microcapsules. Herein, one enzyme unit (1 U) is defined as the production of 1.0 μmol of cholestenone per minute. The test was repeated five times to obtain an average enzyme activity. The immobilization amount (mg/g) of Chox on the microcapsules was calculated through the enzyme activity of the immobilized Chox divided by the enzyme activity of as-received Chox (133 U/mg).

The leakage rate (L_R) of microcapsule samples was determined through an analytical balance method. A microcapsule sample with the given mass was heated at 70 ºC and then weighted at every two hours, and its leakage rate was calculated using the following equation.

$$L_R = \frac{m_0 - m_t}{m_0} \times 100\% \tag{5}$$

where m_0 and m_t are the masses of a microcapsule sample at the initial and arbitrary heating time, respectively. Thermal buffering performance and temperature regulation behavior were investigated using a Testo™ 875–1i versatile thermal imager. A certain amount of microcapsule sample was mildly compressed to form a specimen disc and then placed on a glass dish. The glass dish was heated on a high-precision electronic hot plate at a constant temperature of 70 ºC, followed by natural cooling to room temperature. The surface temperature evolution of the microcapsule sample as a function of time was obtained through infrared thermographic analysis using the Testo™ ComSoft Basic software. The shape/form stability and leak prevention of microcapsule samples was investigated through isothermal heating at 120 ºC on a high-precision electronic hot plate. A digital camera was employed to record the real-time appearances of microcapsule samples and pure *n*-docosane during the isothermal heating process.

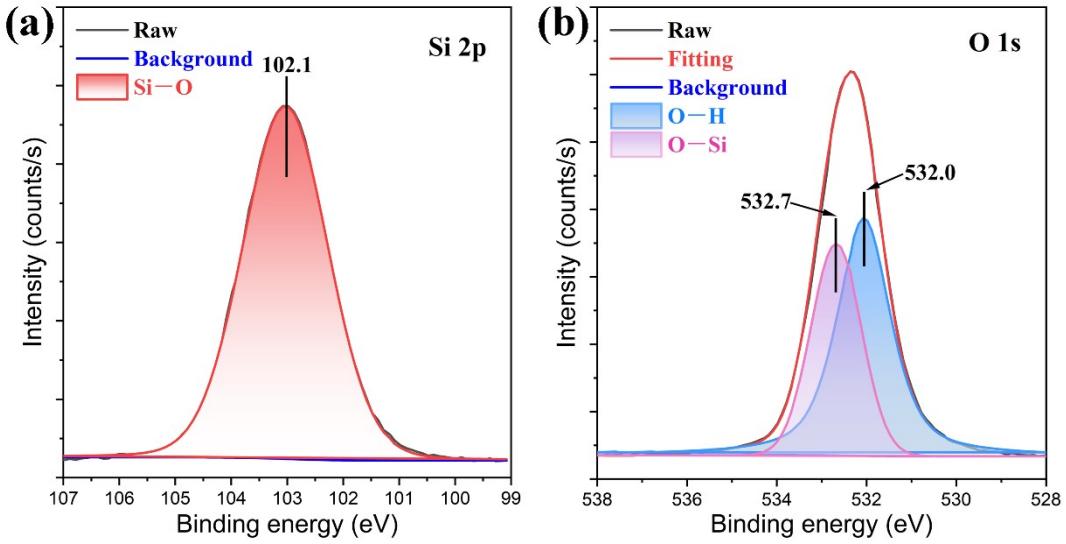

Fig. S1. High-resolution XPS core-level spectra of the SiO_2@*n*-C_{22} MEPCM in specific binding energy of (a) Si 2p and (b) O 1s.

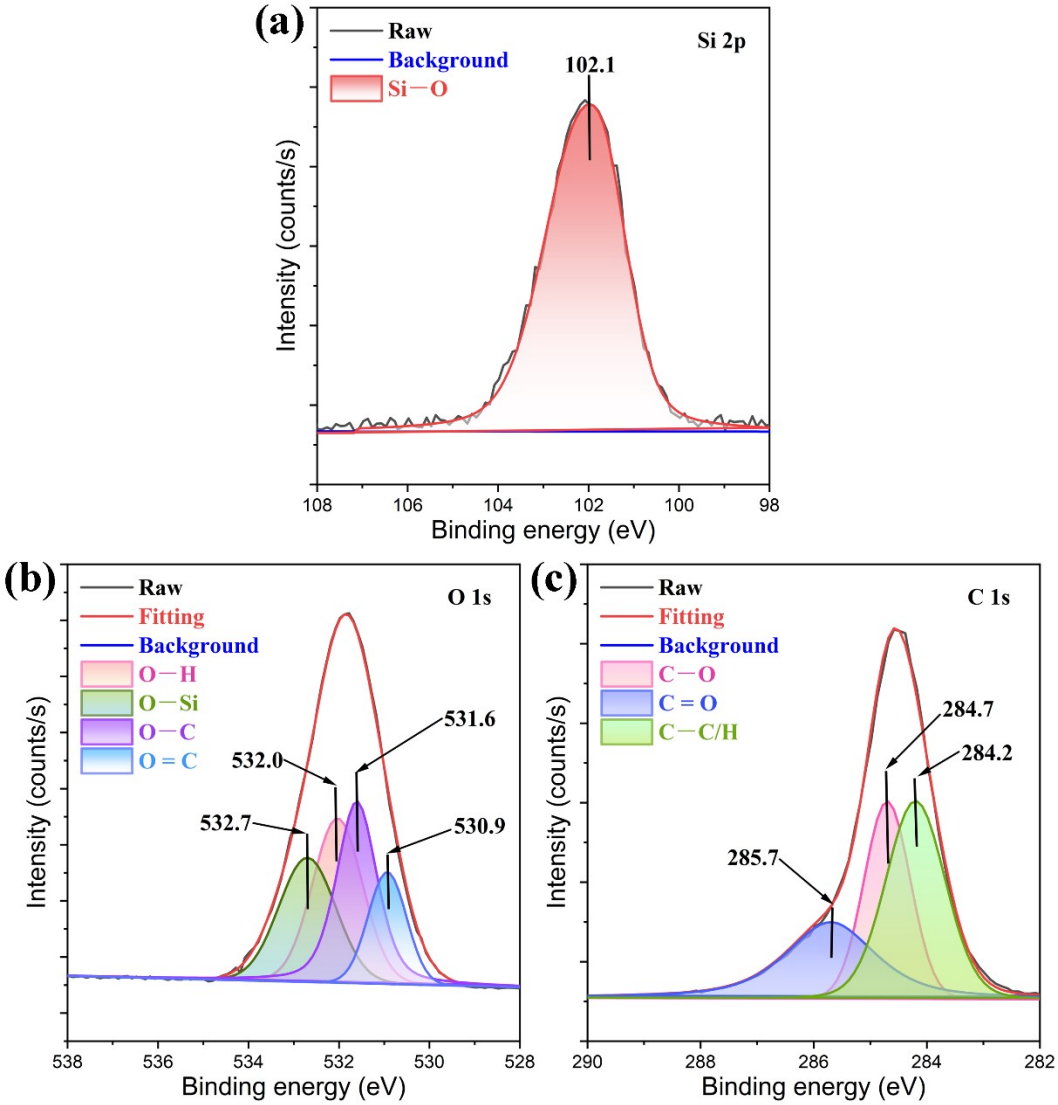

Fig. S2. High-resolution XPS core-level spectra of the SA/SiO_2@*n*-C_{22} MEPCM in specific binding energy of (a) Si 2p, (b) O 1s, and (c) C 1s.

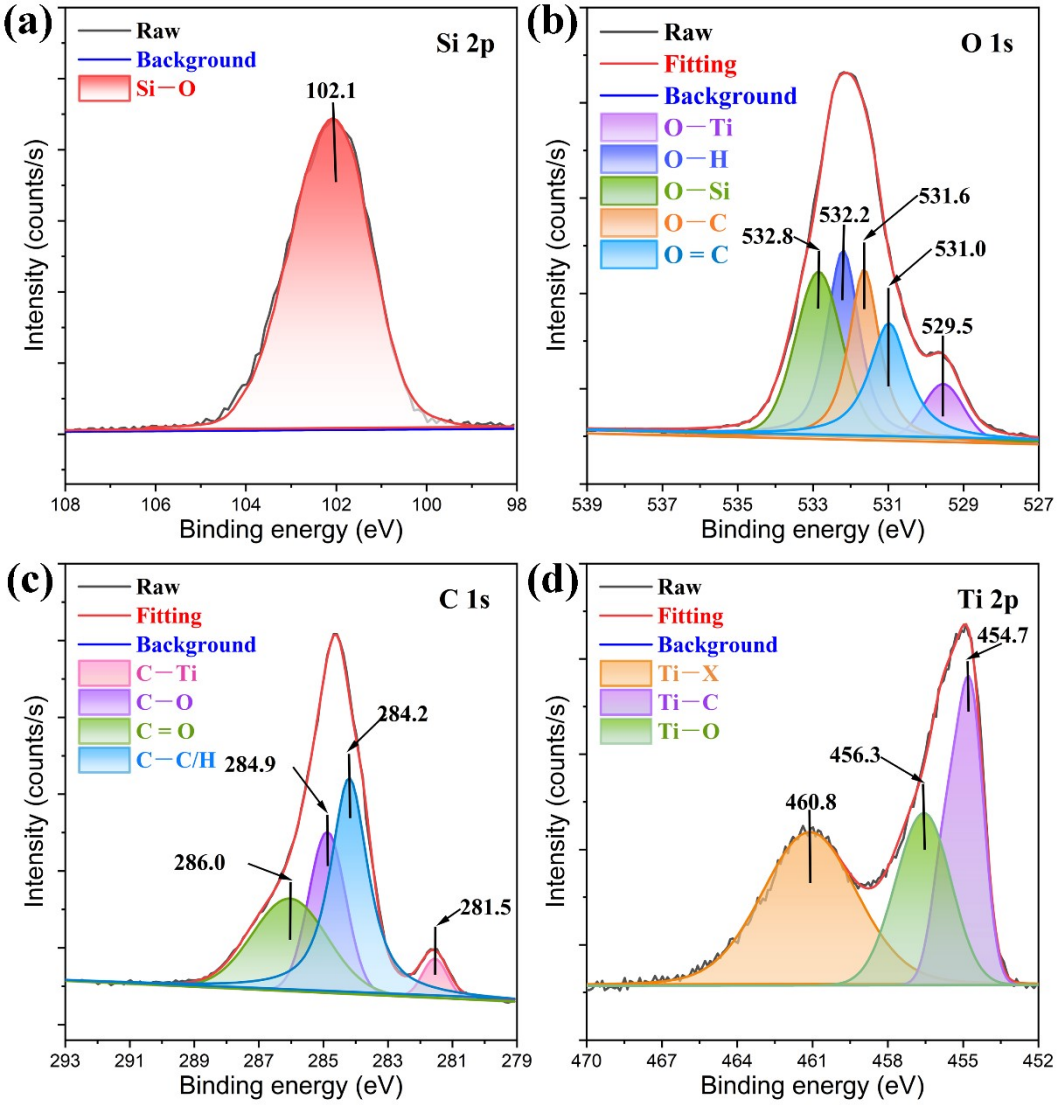

Fig. S3. High-resolution XPS core-level spectra of the MXene/SA/SiO_2@*n*-C_{22} MEPCM in specific binding energy of (a) Si 2p, (b) O 1s, (c) C 1s, and (d) Ti 2p.

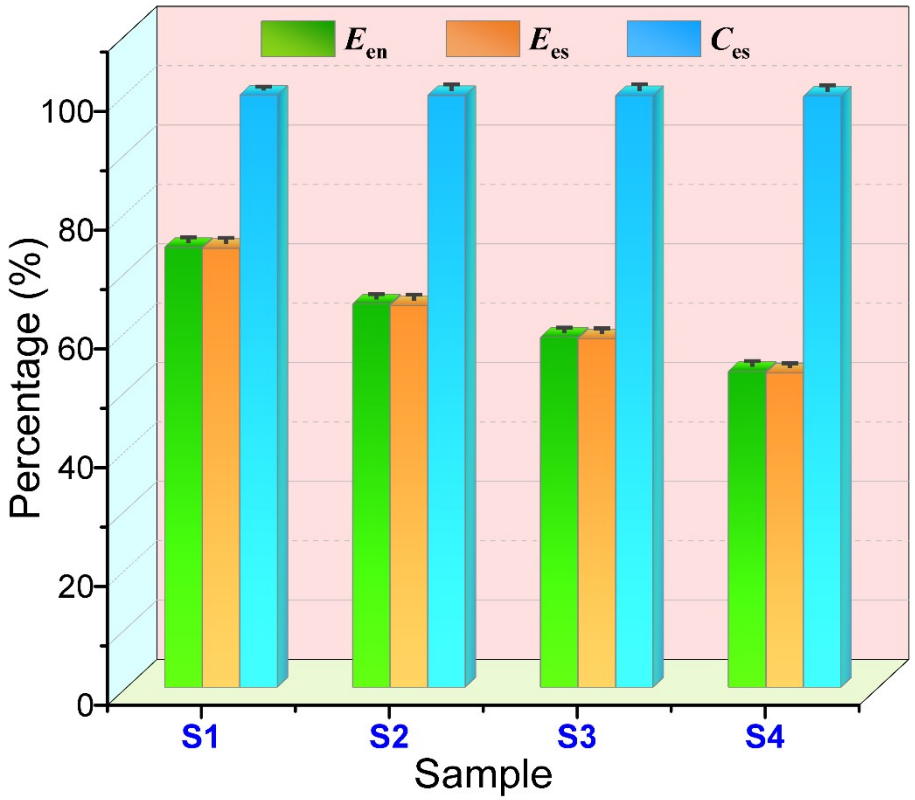

Fig. S4. Encapsulation parameters of (S0) pure *n*-docosane, (S1) SiO_2@C_{22} MEPCM, (S2) SA/SiO_2@C_{22} MEPCM, (S3) MXene/SA/SiO_2@C_{22} MEPCM, and (S4) Chox-MXene/SA/SiO_2@C_{22} MEPCM.

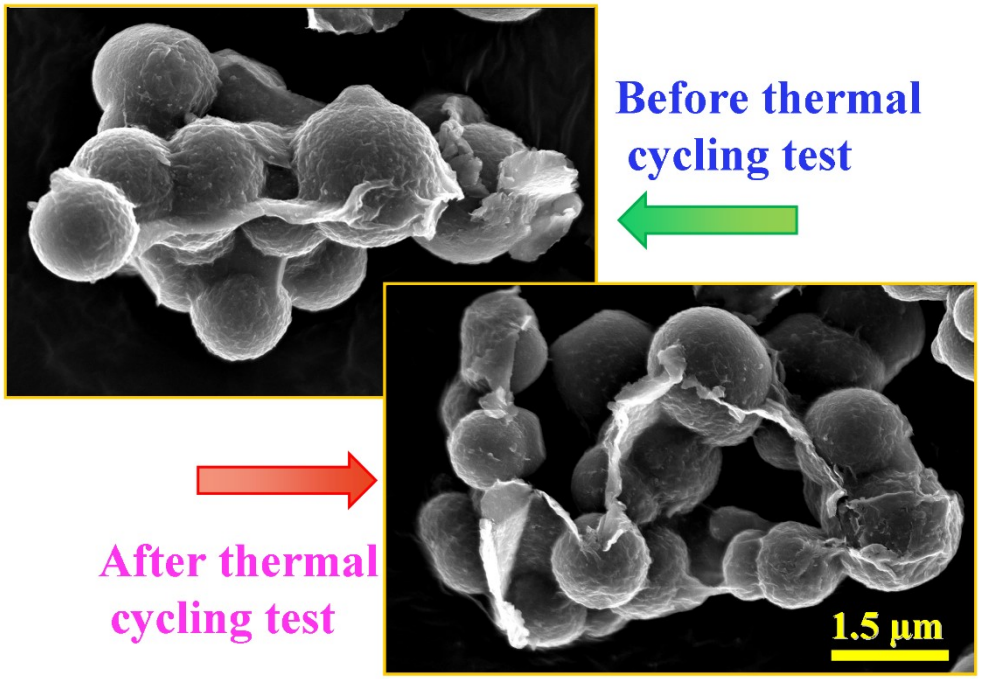

Fig. S5. SEM micrographs of Chox-MXene/SA/SiO_2@C_{22} MEPCM before and after thermal cycling experiment.

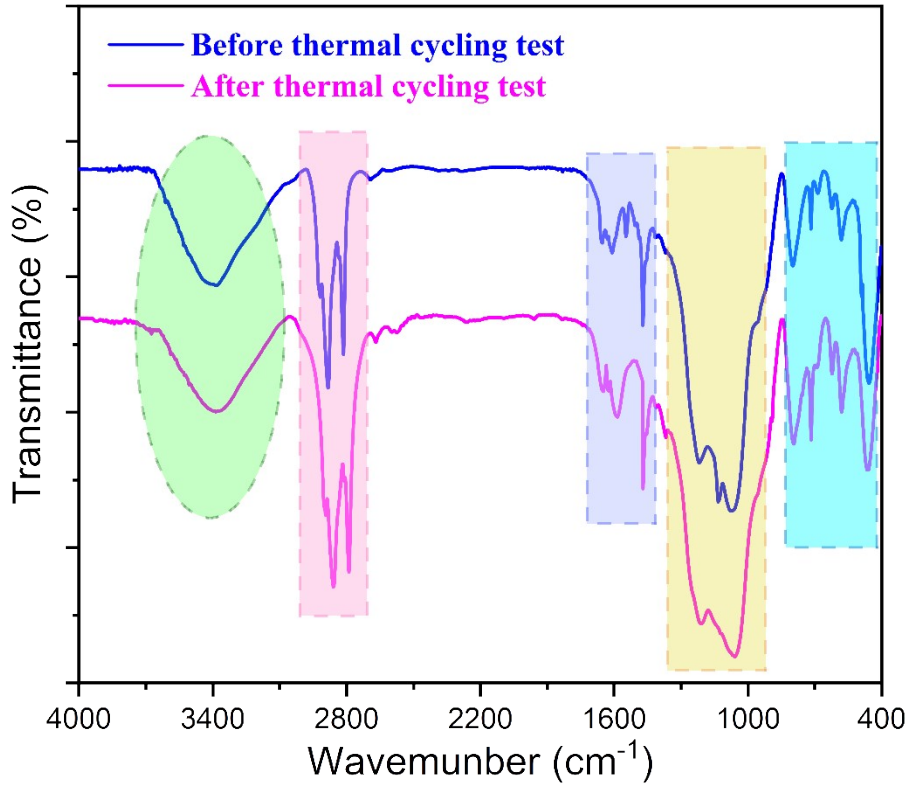

Fig. S6. *FT*-IR spectra of Chox-MXene/SA/SiO_2@C_{22} MEPCM before and after thermal cycling experiment.

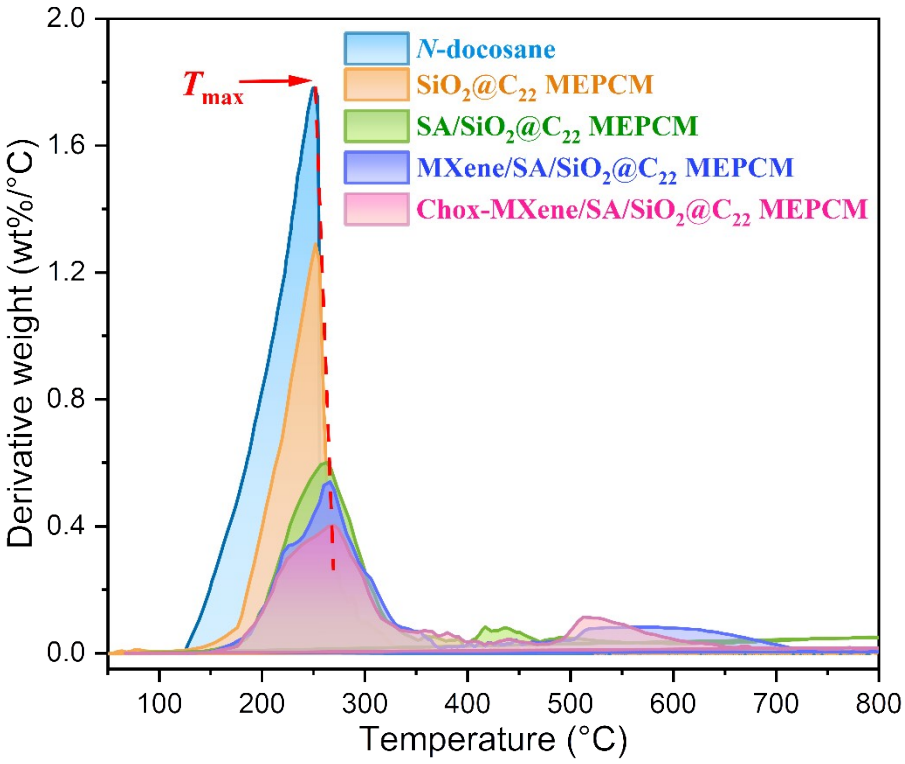

Fig. S7. DTG curves of pure *n*-docosane and microcapsule samples.

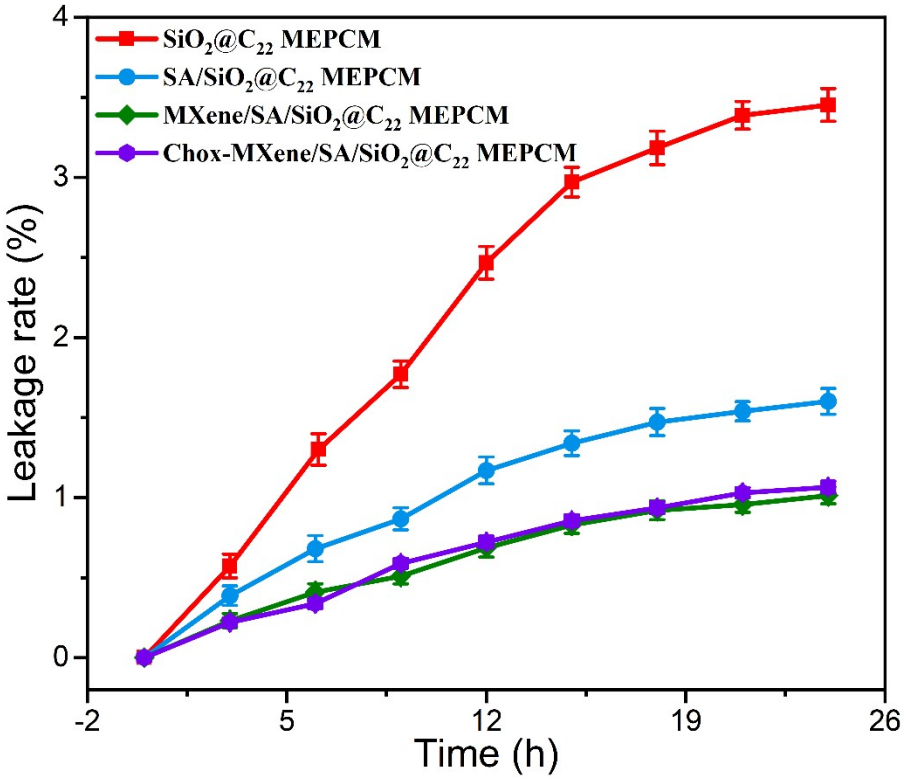

Fig. S8. Plots of leakage rate as a function of time for microcapsule samples.